Received: 19 July 2011,

Revised: 3 October 2011.

Accepted: 4 November 2011,

Published online in Wiley Online Library: 2012

(wileyonlinelibrary.com) DOI: 10.1002/cmmi.492

Mn-loaded apoferritin: a highly sensitive MRI imaging probe for the detection and characterization of hepatocarcinoma lesions in a transgenic mouse model

Simonetta Geninatti Crich^a, Juan Carlos Cutrin^{b,c}, Stefania Lanzardo^b, Laura Conti^b, Ferenc K. Kálmán^{a,d}, Ibolya Szabó^a, Néstor R. Lago^e, Achille Iolascon^f and Silvio Aime^a*

Mn-Apo is a highly sensitive MRI contrast agent consisting of ca. 1000 manganese atoms entrapped in the inner cavity of apoferritin. Part of the metallic payload is in the form of Mn²⁺ ions that endow the nano-sized system with a very high relaxivity that can be exploited to detect hepatocellular carcinoma in mice. Cellular studies showed that Mn-Apo is readily taken up by normal hepatocytes via the ferritin transporting route. Conversely, hepatoma cells (HTC) displayed a markedly reduced ability to entrap Mn-Apo from the culture medium. The i.v. administration of Mn-Apo into C57BL/6J mice resulted in a marked liver tissue hyperintensity in T_1 -weighted MR image 20 min after injection. When injected into HBV-tg transgenic mice that spontaneously develop hepatocellular carcinoma (HCC), Mn-Apo allowed a clear delineation of healthy liver tissue and tumor lesions as hyperintense and hypointense T_1 -weighted MR images, respectively. Immunohistochemistry analysis correlated Mn-Apo cellular uptake to SCARA5 receptor expression. When the MRI contrast induced by Mn-Apo was compared with that induced by Gd-BOPTA (a commercial contrast agent known to enter mouse hepatocytes through organic anion transporters) it was found that only some of the lesions were detected by both agents while others could only be visualized by one of the two. These results suggest that Mn-Apo may be useful to detect otherwise invisible lesions and that the extent of its uptake directly reports the expression/regulation of SCARA5 receptors. Mn-Apo contrastenhanced MR images may therefore contribute to improving HCC lesion detection and characterization. Copyright © 2012 John Wiley & Sons, Ltd.

Keywords: hepatocellular carcinoma; MRI; manganese; molecular imaging; ferritin

1. INTRODUCTION

Hepatocellular carcinoma (HCC) is the fifth most common cancer worldwide, with a median survival time of 6–16 months. Factors responsible for its poor prognosis include late-onset diagnosis, underlying cirrhosis and resistance to chemotherapy (1,2). Magnetic resonance imaging (MRI) has been recognized as an important approach for HCC detection (3,4). Hypervascular lesions are well assessed by contrast-enhanced dynamic MRI in the early arterial phase using Gd-DTPA [diethylenetriamine penta-acetic acid Gd(III) complex] or analogous hydrophilic complexes (5). Conversely, the visualization of nonhypervascular tumors is more difficult. It has been found that, by using Gd complexes bearing a hydrophobic substituent, in the hepatobiliary phase (20 min after contrast agent injection), the liver signal intensity enhancement is directly proportional to the expression of specific transporters that these Gd complexes use to enter hepatocytes (6,7). It has been shown that the uptake of Gd complexes by hepatocytes occurs through organic anion transporters (OATPs) (8–10). Since OATPs expression can be up- or down-regulated in HCCs, the assessment of Gd complexes cellular uptake may be misleading in the detection of tumor lesions. For these reasons, it appears important to exploit additional targets for MRI diagnostic agents on the surface

- * Correspondence to: Silvio Aime, Center for Molecular Imaging, Department of Chemistry IFM, University of Turin, Turin, Italy. E-mail: silvio.aime@unito.it
- a S. Geninatti Crich, F. K. Kálmán, I. Szabó, S. Aime Center for Molecular Imaging, Department of Chemistry IFM, University of Turin, Turin, Italy
- b J. C. Cutrin, S. Lanzardo, L. Conti Department of Clinical and Biological Sciences, University of Turin, Turin, Italy
- J. C. Cutrin
 ININCA-CONICET (National Council of Scientific and Technical Reserch of Argentina),
 Buenos Aires, Argentina
- d F. K. Kálmán Department of Inorganic and Analytical Chemistry, University of Debrecen, Debrecen, Hungary
- e N. R. Lago Center of Experimental Pathology, School of Medicine, University of Buenos Aires, Buenos Aires, Argentina
- f A. Iolascon CEINGE Biotecnologie Avanzate, University of Naples, Naples, Italy

of normal hepatocytes or HCC cells in order to pursue an early and more accurate characterization of liver cancer.

Iron required for normal cell function, enzymatic reactions and heme biosynthesis is provided by circulating holo-transferrin that binds to cell surface receptors and is internalized by endocytosis (11). However, evidence has been gained to support the view that mammalian cells can also acquire iron via transferrinindependent pathways (12). In kidney organogenesis a novel receptor, the scavenger receptor member 5 (SCARA5), has been identified as a receptor for L-ferrritin which mediates the delivery of nontransferrin-bound iron to the developing kidney (13,14). Furthermore, in a clinical oncology study, Huang and co-workers reported the relationship between SCARA5 expression and HCC aggressiveness (15). They found that SCARA5 down-regulation was associated with cellular invasion, venous permeation and metastasis. Furthermore, in vitro SCARA5 knockdown experiments have shown that the lack of this protein leads to a marked enhancement in HCC cell growth and of invasiveness, tumorigenicity and lung metastasis when such cells are injected into nude mice (15).

The aim of this work was to assess whether Mn-loaded L-apoferritin (Mn-Apo) can act as an MR molecular imaging reporter of SCARA5 expression. The fulfillment of this task will open new possibilities to visualize the progressive down-regulation of SCARA5 during the evolution of transformed cells in dysplastic/neoplastic nodules. This MRI contrast agent is a highly sensitive system containing a large number of paramagnetic Mn(II) aquaions entrapped in the inner cavity of apoferritin (16). The preparation of Mn-Apo relies on the dissolution of the previously formed β -MnOOH inorganic phase that occurs via the reduction of Mn(III) to Mn(III) operated by aminopolycarboxylic acids that also act as sequestering agents for the weakly coordinated manganese ions on the outer surface of the protein (Fig. 1A). The reductive treatment allowed generation of an apoferritin-based nanocarrier (Mn-Apo) containing up to 300–400 Mn(III) aquaions encapsulated

in the inner cavity. This procedure yields to the attainment of a MRI agent endowed with a remarkably high relaxivity value (per apoferritin) of about 7000 mm⁻¹ s⁻¹. In this work the high sensitivity of Mn-loaded apoferritin has been exploited to investigate its capability to discriminate between hepatic dysplastic/ neoplastic lesions and normal parenchyma both in vitro and in HCC-developing HBV-Tg mice. HBV-Tg mice, officially designed as Tg (Alb-1HBV) Bri44¹⁷, which express the HBV genomic sequence for pre-S, S and X proteins, appear to be an ideal model for the characterization of the steps that leads to HCC (17-19). In fact these Tg mice develop progressive hepatocyte damage that determines degenerative alterations in the first month of life followed by elevated damage-related compensatory proliferative and precancerous response after the ninth month of life, followed by the appearance of dysplastic hepatic lesions, which become clearly neoplastic after the twelfth month. Successively, neoplastic lesions progressively grow to macroscopic nodules that can be observed in all animals within the sixteenth to eighteenth month of life.

2. RESULTS

2.1. In Vitro Studies of Mn-Apo Uptake in Rat Hepatocytes and Hepatoma Cells

The uptake of Mn-Apo was investigated on both rat hepatocytes and HTC cells. The efficiency of Mn-Apo in entering cells was evaluated by acquiring T_1 -weighted spin-echo images of cellular pellets on a 7 T MRI scanner. Figure 1(B) shows that the internalization of Mn-Apo is markedly more efficient in healthy hepatocytes with respect to hepatoma. In fact there is a large difference in the measured relaxation rates (Fig. 1C) that is clearly reflected in the T_1 -weighted images. The viability of the cells labeled with Mn-Apo (96 \pm 3 and 80 \pm 5% for HTC and hepatocytes, respectively) was not significantly different from control cells (97 \pm 3 and 78 \pm 5% for HTC and hepatocytes, respectively). HTC competition studies

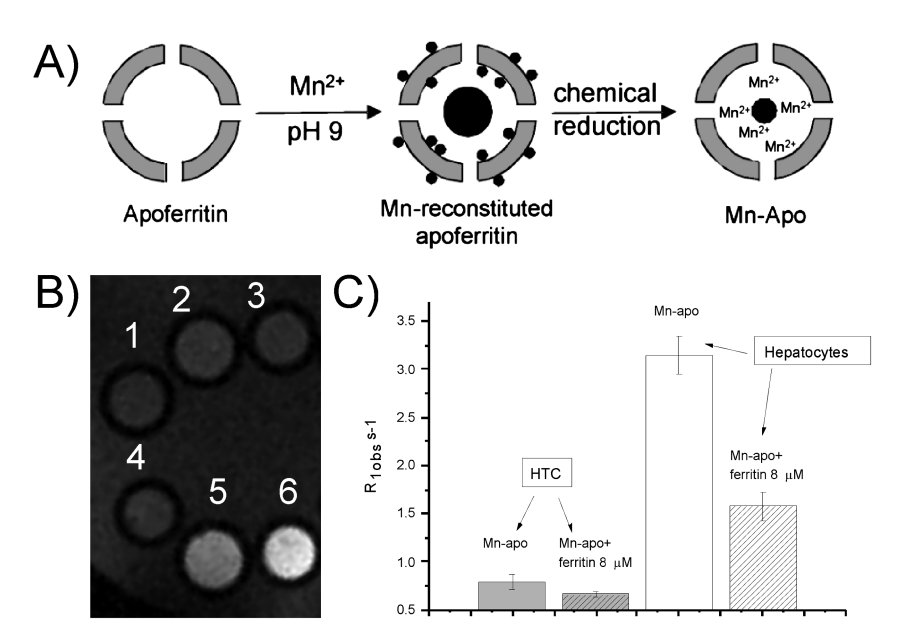


Figure 1. Mn-Apo uptake by hepatocytes and hepatoma cells. (A) Schematic representation of the Mn-Apo preparation. (B) T_1 -weighted spin echo MR image (7T) of an agar phantom containing: unlabeled HTC (1); HTC incubated with Mn-Apo at 0.2 mm Mn concentration in the absence (2) and in the presence (3) of an excess (7.2 mg) of native ferritin; unlabeled hepatocytes (4); hepatocytes incubated with Mn-Apo at 0.2 mm Mn concentration in the presence (5) and in the absence (6) of an excess (7.2 mg) of native ferritin; (C) Relaxation rates of the Mn-containing cell pellets (the same as in B) measured at 7T using a standard saturation recovery sequence. Error bars indicate mean \pm SD.

with native ferritin confirmed that the cellular uptake of Mn-Apo involves ferritin receptors in both hepatocytes and hepatoma cells (Fig. 1B and C).

2.2. In Vitro MRI on C57BL/6 Mice

In order to assess the biodistribution of Mn-Apo imaging probes in mice, a group of C57BL/6 wild-type mice were injected with a solution of this agent to reach the Mn dose of 0.01 mmol kg⁻¹. As shown in Fig. 2(A), a very high SI enhancement of the liver was detected 20 min after Mn-Apo administration. After 24 h, the effect had almost completely disappeared.

Recently, Li *et al.* reported SCARA5 as a receptor for L-ferritin, which appears to be able to mediate the delivery of nontransferrinbound iron in different epithelial cells (13). In order to assess if this receptor could be involved in Mn-Apo uptake, SCARA5 expression on normal liver was evaluated by immunoistochemistry. As reported in Fig. 2(B), hepatocytes showed a positive granular reaction at the plasma membrane level with a slight diffusion over the cytosol. There was not an acinus (ellipsoidal mass of hepatocytes aligned around the hepatic arterioles and portal venules) predominance in the presence of SCARA5.

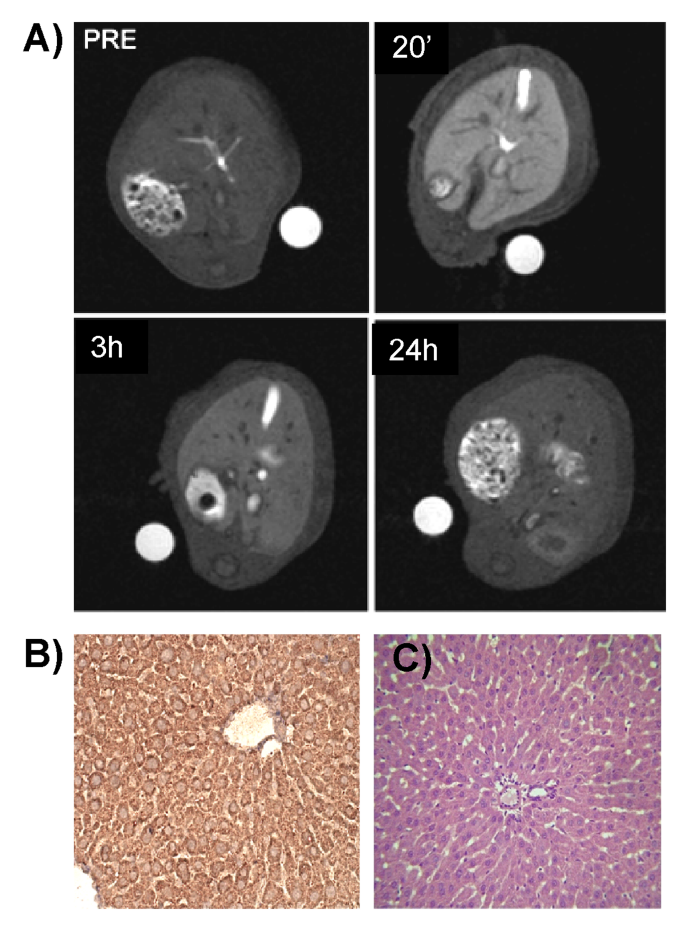


Figure 2. *In vivo* MRI on C57BL/6 mice. (A) T_1 -weighted MR images of C57BL/6 mice (liver region) acquired before and 30 min, 3 h and 24 h after the administration of Mn-Apo at an Mn dose of 0.01 mmol kg $^{-1}$. (B) Immunohistochemistry; plasma-membrane positive reaction for SCARA5 in hepatocytes from an age-matched wild-type mouse (×200, counterstained with hematoxylin); (C)nNormal liver hepatocytes (200× hematoxylin–eosin).

In order to prove that Mn-Apo is specifically internalized through liver ferritin receptors, a competition study with native ferritin was performed by injecting 2.5 mg of the protein 1 h before the injection of Mn-Apo (0.01 mmol kg⁻¹). Table 1 shows that liver uptake of Mn-Apo is markedly reduced by the saturation of the receptors with an excess of native ferritin. Under these conditions the amount of Mn-Apo excreted by kidneys increases whereas the spleen uptake appears negligible. The absence of spleen uptake outlines the fact that Mn-Apo is not a target of the reticuloendothelial system (Table 1).

2.3. In Vitro MRI on HBV-Tg Mice

HBV-Tg transgenic mice (13 months old), a well-established animal model for hepatocarcinogenesis, were used to evaluate the ability of Mn-Apo to discriminate between normal liver and neoplastic lesions. MR images were acquired 20 min after injection of Mn-Apo (0.01 mmol kg⁻¹ Mn). Figure 3 shows MR images of HBV-Tg mice livers, characterized by hypointense lesions as a consequence of a reduced uptake of the imaging probe. A total number of 16 lesions were detected for the six screened mice. On the basis of SNR (signal to noise ratio) and CNR (contrast to noise ratio) analysis, the detected lesions were assigned to three groups with decreasing signal intensity (SI) on going from type I to type II to type III (Table 2). Only lesions type II and type III were found to be significantly different from normal liver.

In order to compare the diagnostic potential of Mn-Apo with currently used MRI hepatotropic contrast agents, the same group of mice was treated, three days later, with Gd-BOPTA (gadobentatedimeglumine), which is known to be efficiently taken up by healthy mice hepatocytes through OATP transporters (20). A 3 day interval has been selected in order to assure the complete clearance from the liver of the previously injected Mn-Apo. Interestingly, in Gd-BOPTA enhanced MRI, some of the lesions appeared hypointense with respect to the normal liver, showing a direct correspondence with that observed in Mn-Apo-enhanced images (Fig. 3, lesions 2 and 6). Of the remaining lesions, six were undetectable with Gd-BOPTA because they were isointense with respect to normal hepatic tissue (Fig. 3, lesions 3 and 4), whereas a third group of them were hypointense only in Gd-BOPTA and not in Mn-Apo-enhanced images (Fig. 3, lesions 1 and 5). The comparison between Mn-Apo and Gd-BOPTA was also carried out 1 h time after contrast administration without observing any significant difference from the results obtained at 20 min.

The macroscopic appearance of explanted liver from HBV-Tg mice showed multifocal and sometimes multinodular tumors growth. Liver tumors displayed both intra- and inter-individual heterogenicity. Tumors displaying the cytological and histological characteristics typical of clear-cell adenomas and carcinomas were found. In many nodules diagnosed as hepatocellular carcinomas, diffuse fat change, conspicuous mitosis, eosinophilic cytoplasmic bodies and a disorganized pattern of blood vessels were frequently observed (Fig. 4). No signs of necrosis were evident. Wild-type age-matched mice had a normal liver aspect.

SCARA5 was evaluated by immunohistochemistry in liver from HBV-Tg and age-matched wild-type mice. An intense plasma membrane granular positive reaction with cytoplasmic diffusion was evident only in the normal and noncancerous hepatic parenchymal cells (Fig. 2B). In contrast, neoplastic cells displayed a heterogeneous reaction (Fig. 4). In other terms, some cancerous lesions were characterized by a markedly positive reaction in all their cellular components (Fig. 4C), whereas other carcinomas

Table 1. MRI% signal intensity enhancement measured on liver, spleen, kidneys, muscle, with or without ferritin pre-injection. Data are reported \pm SD

Time after Mn-Apo injection	Liver SI enhancement (%)	Spleen SI enhancement (%)	Kidneys SI enhancement (%)	Muscle SI enhancement (%)
0.5 h without ferritin pre-injection	86 ± 4	3 ± 0.15	57 ± 3	8.5 ± 0.4
0.5 h with ferritin pre-injection	37 ± 4	2.5 ± 0.2	70 ± 4	4 ± 1.5
3 h without ferritin pre-injection	49 ± 3	0.3 ± 0.2	52 ± 3	2 ± 0.1
3 h with ferritin pre-injection	26 ± 3	0.4 ± 0.1	66 ± 3	8 ± 1.5
20 h without ferritin pre-injection	6 ± 0.3	0.2 ± 0.1	10 ± 0.5	0.4 ± 0.2
20 h with ferritin pre-injection	1 ± 0.5	0 ± 0.6	24 ± 2	2 ± 2

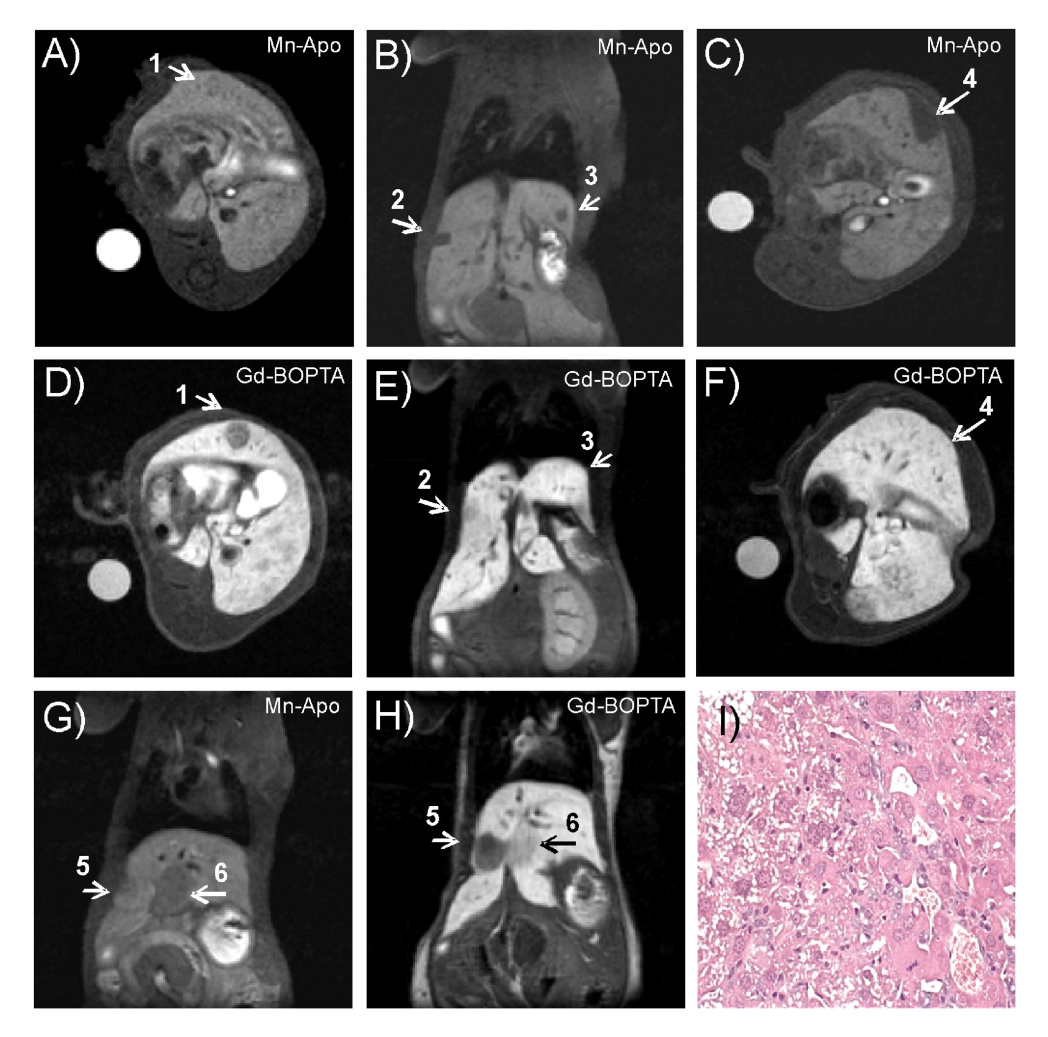


Figure 3. In vivo MRI on HBV-Tg mice. T_1 -weighted MR images (liver region), recorded at 7T, of HBV-Tg transgenic mice 20 min after the injection of Mn-Apo (A, B, C, G) and Gd-BOPTA (D, E, F, H), respectively. Neoplastic lesions were indicated by growing numbers. Lesions 1 and 5 were hypointense with respect normal liver only after Gd-BOPTA administration, but lesions 3 and 4 only after Mn-Apo injection. Lesions 2 and 6 were hypointense with both contrast agents. (I) Hepatocelular carcinoma in a 13-month-old HBV-Tg transgenic mouse (\times 200 hematoxylin-eosin).

Table 2. Comparison of SNR and CNR measured on different HBV-Tg tumor lesions 20 min after the injection of Mn-Apo						
	Normal Liver	Type I lesions	Type II lesions	Type III lesions		
SNR CNR	30 ± 2.6 -0.37 ± 2.8	$28.4 \pm 2.6 \ (p = 0.6474)$ $-2.8 \pm 1.0 \ (p = 0.0192)$	$22.8 \pm 1.5 \; (p < 0.0001) \\ -6.5 \pm 1.1 \; (p < 0.0001)$	$14.4 \pm 1.4 \; (p < 0.0001) \\ -11.8 \pm 1.7 \; (p < 0.0001)$		
SNR, signal-to-noise ratio; CNR, contrast to noise ratio.						

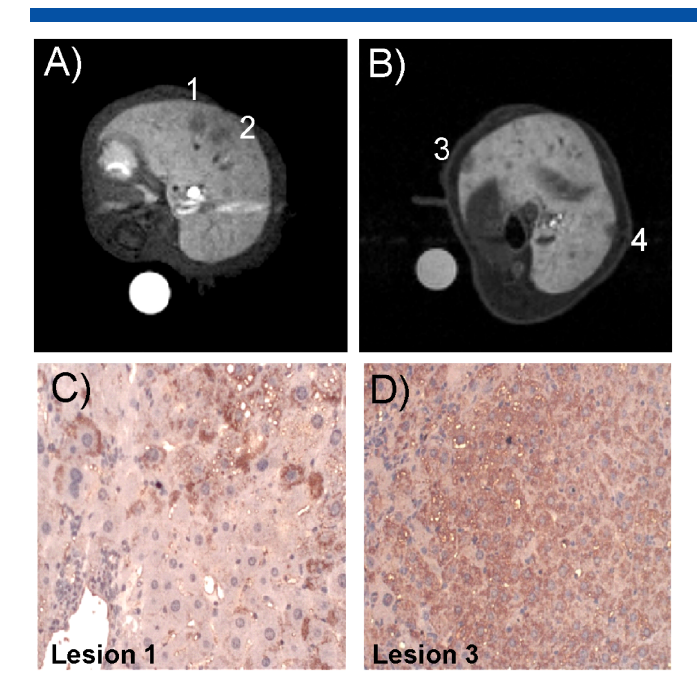


Figure 4. Histological validation of MRI lesion detection. T_1 -weighted MR images (liver region), of HBV-Tg transgenic mice 20 min after the injection of Mn-Apo (A) and Gd–BOPTA (B), respectively. Lesions 1 and 2 were easily detectable only after Mn-Apo administration. However, lesions 3 and 4 were detectable only after Gd–BOPTA injection. (C, D) Expression pattern of SCARA5 in HBV-Tg. (C) Immunohistochemical staining of lesion 1 showing low Mn-Apo uptake. SCARA5 was observed only in some tumor cells (\times 200, counterstained with hematoxylin). (D) Immunohistochemical staining of lesion 3 showing higher Mn-Apo uptake. SCARA5 was present in almost all cancer cells (\times 200, counterstained with hematoxylin).

exhibited a mosaic-like pattern in which areas of positive and negative neoplastic cells were mixed (Fig. 4D). Interestingly, neoplastic lesions hypointense in Mn-Apo-enhanced MR images corresponded to lesions with a lower SCARA5 expression, thus indicating a good correspondence between MRI and immunohistochemistry results.

The potential toxicity of the Mn-Apo to the liver was evaluated in terms of alanine aminotransferase (ALT) activity in serum. Four wild-type mice (13 months old) were treated with Mn-Apo (0.01 mmol $kg^{-1}\,$ Mn). After, 24 h serum samples were collected and ALT activity was assessed and compared with the one measured for four untreated wild-type mice. The measured ALT activity was 38 ± 6 and 40 ± 10 U I $^{-1}$ for Mn treated and untreated mice, respectively. These values demonstrate the absence of liver damage owing to Mn containing contrast media exposure. The complete elimination of the Mn from the liver was checked by inductively plasma mass spectrometry (ICP-MS) 24 h after Mn-Apo administration on both wild-type and HBV mice. Table 3 shows that the Mn level measured 24 h after Mn-Apo injection was not significantly different from the basal Mn concentration found in the liver parenchimas of untreated wild-type and HBV mice.

3. DISCUSSION

The major aim of this study deals with the design of a noninvasive imaging protocol that could potentially contribute to the improvement of human hepatocellular carcinoma diagnosis. In fact, the

Table 3. Liver Mn concentration measured by ICP-MS of both wild-type and HBV mice with or without Mn-Apo administration (0.01 mmol ${\rm kg}^{-1}$ Mn). Mn concentration was measured 24 h after the contrast agent injection

	Liver [Mn], ng g ⁻¹ , wild-type mice	Liver [Mn], ng g ^{–1} , HBV mice
Untreated	$\textbf{1.1} \pm \textbf{0.16}$	$\textbf{1.24} \pm \textbf{0.05}$
Mn-Apo treated (24 h)	1.23 ± 0.18	1.03 ± 0.3

noninvasive detection and characterization of hepatic lesions is still an issue in spite of the efforts with different diagnostic imaging modalities (21,22). In the last 10 years attention has been focused on two liver-specific MRI contrast media, namely Gd-EOB-DTPA (gadolinium ethoxybenzyl diethylenetriaminepentaacetic acid) and Gd-BOPTA. They can be used either in the early dynamic phase, as standard Gd agents, or in the hepatobiliary phase, where some hepatic lesions appear hypo-intense with respect to the normal tissue as a consequence of the lower uptake of the contrast media, whereas other metastatic lesions appear iso- or hyperintense. This is the consequence of the different expression of OATP transporters that has been shown to be not directly related to tumor differentiation (9). Targeting others biomarkers may allow an improved characterization of the cellular transformations that lead to HCC. Since the epitopes to be targeted are usually present at very low concentrations, it is necessary to design proper methods to amplify the MRI response (23,24).

Ferritin is an interesting carrier for molecular imaging agents since its internal cavity, once deprived of the iron core, can be loaded with manganese ions or Gd complexes to yield a system endowed with high T_1 relaxation enhancement capability (16,25–27). The loading with paramagnetic ions does not modify the external structure of the protein assembly, maintaining unaltered the affinity for its receptors, whose expression can change upon the development of hepatic disease. Li et al. (13) identified SCARA5 as a receptor for L-ferritin that mediates the delivery of nontransferrin-bound iron to the developing kidney. In liver, SCARA5 down-regulation appears related to HCC tumorigenesis and metastasis (15). On the basis of these considerations, SCARA5 can be proposed as a molecular marker of HCC and its expression can be followed using Mn-Apo as a noninvasive MRI reporter. In fact, the lower uptake of Mn-Apo into hepatoma cells with respect to healthy hepatocytes allows good discrimination between the two cell types. Mn-Apo injected intravenously at the same dose of the clinically approved Mn-DPDP (Teslascan) (28,29) is very efficiently taken up by liver, and the extent of its uptake depends on ferritin receptor expression. Herein it has been shown that, after administration of Mn-Apo to 13-month-old HBV-Tg, the contrast in MR images is hypointense in the liver regions histologically corresponding to hepatocarcinoma. About 60% of these lesions are also detectable in Gd-BOPTA-enhanced images, but the remaining ones appear isointense with respect to the surrounding normal liver tissue. Conversely, of the 16 lesions detected in Gd-BOPTA-enhanced images, six of them are not visible in Mn-Apo enhanced images. This is consistent with the fact that SCARA5 expression is not uniform in all types of clinical hepatocellular carcinomas (15). In correspondence, we have shown, in this experimental model of hepatocarcinogenesis, that some nodules had a nonhomogenous distribution of SCARA5. However, from these preliminary results, in which only an endpoint of mouse life-span was evaluated, we cannot assess whether the down-regulation of SCARA5, observed in some tumors lesions, could be playing a major role during the multistep process of neoplastic transformation, as Huang *et al.* have proposed (15). In their paper, the authors discovered a direct association between SCARA5 down-regulation and the more aggressive clinical behavior of human HCC that led them to suggest SCARA5 as an oncosuppressor molecule.

The heterogeneity (30) in the expression of different receptors/ transporters on cell surfaces in hepatic lesions outlines the importance of the use of different contrast agents, internalized through different pathways, in order to improve the diagnosis of this complex pathology. The herein reported investigations give important insights to correlate the ferritin receptors expression to the neoplastic evolution of HCC. As a final remark, we think that the Mn-Apo system investigated may have diagnostic applications well beyond liver-related diseases. Manganese is an essential metal in living systems and it may represent a viable alternative to Gd as cells have set up well-established storing/excretion pathways for controlling its homeostasis. The administration of Mn(II) agua ions well confined within the ferritin inner cavity appears to be an efficient method to conjugate low toxicity with high efficacy. Furthermore, apoferritin does not stimulate any immune reaction, thus allowing for the design of probes that may stay in circulation for a time sufficiently long for specific targeting needs typical of molecular imaging diagnostic procedures.

4. EXPERIMENTAL

4.1. Preparation of Mn-Reconstituted Apoferritin

The Mn-Apo preparation was carried out as described previously (16). Briefly, iron-free horse spleen apoferritin (Sigma-Aldrich, Co., St Louis, MO, USA) was reconstituted in the presence of MnCl₂ solution at pH = 9.0, under air. To avoid the fast oxidation of the Mn(II) ion, the apoferritin and Mn(II) were added into an N₂-saturated AMPSO [*N*-(1,1-dimethyl-2-hydroxyethyl)-3-amino-2-hydroxypropanesulfonic acid, Fluka, Milan, Italy] solution, which had been previously corrected to the desired pH. The protein and the Mn(II) solutions were added to reach 1×10^{-6} and 3×10^{-3} M concentration, respectively, corresponding to a loading of 3000 Mn(II) ions per apoferritin molecule. After 1 week reaction time, the samples were treated for 4h at 20°C with TETA (1,4,8,11-tetraazacyclotetradecane-1,4,8,11-tetraacetic acid, Fluka, ≥97%) to reduce Mn(III) to Mn(II) as well as to remove Mn(II) ions bound at the outer surface of the protein shell. The obtained Mn-Apo solutions were characterized in terms of protein concentration by means of the Bradford method (31), using bovine serum albumin (BSA, Sigma-Aldrich, Milan, Italy) as a standard. The metal concentration was determined by adding the same volume of HCl 37% and left at 120 °C overnight. Upon this treatment, all Mn^{II,III} was solubilized as free Mn(II) agua ions. The method was double-checked by ICP-MS measurements. By measuring the water proton relaxation rate of these solutions, it was possible to determine their concentration (16).

4.2. Cell Cultures

The culture media DMEM F-12 (Dulbecco's modified Eagle medium, Nutrient Mixture F-12), M199 (medium 199) and FBS (fetal bovine serum) were purchased from Cambrex (East

Rutherford, NJ, USA). The penicillin–streptomycin mixture, BSA, trypsin, glutamine and all other chemicals were from Sigma Chemical Co. (St Louis, MO, USA). Rat hepatocytes were isolated using a previously reported method (32). HTC (rat hepatoma tissue culture, ATCC, Manassas, VA, USA) were grown in DMEM F-12 medium supplemented with 5% FBS, 2 mm glutamine, 100 U ml $^{-1}$ penicillin and 100 μ g ml $^{-1}$ streptomycin. HTC were cultured in 75 cm 2 flasks in a humidified incubator at 37 °C and at CO $_2$ /air.

4.3. Uptake Experiments

HTC and hepatocytes were seeded at a density of 2.8 and 7.0×10^4 cells cm $^{-2}$, respectively. The trypan-blue exclusion test was used to assess cell viability. At 24 h after seeding, cells were washed three times with PBS and incubated at 37 °C and 5% CO $_2$ for 2 h in the presence of Mn-Apo 0.2 mM in 2 ml of fresh medium. For competition tests 7.2 mg of native ferritin were added to the cell culture medium 1 h before Mn-Apo addition. At the end of incubation, cells were washed three times with ice-cold PBS (phosphate buffer saline), detached with trypsin–EDTA, and transferred into glass capillaries for MRI analysis. The protein concentration of cellular pellets was determined from cell lysates by the Bradford method (31).

4.4. Animals

Twelve-week old male C57BL/6 J (wild-type) mice were purchased from Charles River Laboratories Italia (Calco, Italy) and 12-week-old HBV-Tg male mice were gently provided by Professor Iolascon (CEINGE University Federico II, Naples, Italy). All mice were bred and maintained in specific pathogen-free conditions in the animal facility of the Clinical and Biological Sciences Department, University of Turin, Italy. Their handling and all manipulations were carried out in accordance with the European Community guidelines, and all the experiments were approved by the Ethical Committee of the University of Turin.

4.5. Morphological Analysis

Both Tg and wild-type age-matched mice (52 weeks old) were sacrificed by cervical dislocation. In order to obtain tissues sections corresponding to the MRI slices, much care was devoted to maintain the orientation of the liver lobes, relative to the longitudinal, transversal and sagittal axis corresponding to the original in vivo orientation. Liver samples were fixed in 4% paraformaldhyde-lysine-sodium periodate solution in 0.1 M Sorrensons phosphate buffer (pH 7.4) overnight at 4 °C and then embedded in paraffin or cryopreserved in 10, 20 and 30% sucrose solution in 0.01 M TBS (tris buffer solution, pH 7.6). Five-micrometer slices from paraffin-embedded or cryoprotected sections were stained with hematoxylin and eosin to perform histopathology. SCARA5 was evaluated by immunohistochemistry. Briefly, endogenous peroxidase was blocked by incubation of 4 µm de-waxed sections in 0.3% hydrogen peroxide solution in 70% methanol in 0.05 M TBS (pH 7.6) 30 min at room temperature. Then, wet heat-induced epitope retrieval was performed in a mixture of 0.1 m Tris and 0.01 m EDTA solution at pH 9.0 for 20 min and the sections were incubated with a rabbit polyclonal antibody to SCARA5 (Abcam, Cambridge, UK) for 1 h at room temperature. Then, the slides were treated with a horseradish peroxidase-conjugated polyclonal goat anti-rabbit immunoglobulins antibody (Dako, Glostrup, Denmark) 1h at room temperature. Finally, the sections were reacted with the Dako liquid diamonobenzidine-substrate chromogen system and counterstained with hematoxylin. Negative control slides were treated by incubation with TBS instead of the primary antibody, whereas normal livers were used as positive controls. ALT activity was assessed using a commercial kit (Instrumentation Laboratory, Milano, Italy).

4.6. MRI

MR images were acquired on a Bruker Avance 300 spectrometer (7 T) equipped with a Micro 2.5 microimaging probe. The system is equipped with two birdcage resonators with 30 and 10 mm inner diameter, respectively.

4.7. In Vitro

The glass capillaries containing about 2×10^6 cells were placed in an agar phantom, and MR imaging was performed using a standard T_1 -weighted spinecho sequence (repetition time/echo time/number of experiments, 200/3.3/16; field of view, 1.2 cm; one slice, 1 mm; in-plane resolution, $94\times94\,\mu\text{m}$). T_1 measurements of cells were carried out by using a standard saturation recovery sequence.

4.8. In Vivo

C57BL/6 mice (n=8) and HBV-Tg transgenic mice (n=6) were anesthetized by injecting with a mixture of tiletamine-zolazepam (Zoletil 100), $20 \text{ mg kg}^{-1} + \text{xylazine}$ (Rompun) 5 mg kg^{-1} . Four wild-type mice received through the tail vein 3–5 mg kg⁻¹ Mn-Apo (0.01 mmol kg⁻¹ of Mn), whereas another four mice received ferritin (2.5 mg per mouse) 1 h before administration of the same dose of Mn-Apo. Thirteen-month-old HBV-Tg mice (n=6) were i.v. injected with Mn-Apo at the same concentration used above and 3 days later with Gd-BOPTA (MultiHance, Bracco, Milan, Italy) using the clinical dose of 0.1 Gd mmol kg⁻¹. MRI images of C57BL/6 wild-type mice were acquired, 20 min, 3 h and 24 h after the contrast agent administration. MRI images of HBV transgenic mice were acquired before contrast agent administration and 20 min and 1 h after. A T_1 -weighted, fatsuppressed, multislice multiecho protocol (repetition time/echo time/number of experiments, 250/3.2/6; field of view, 3 cm; 1 slice, 1 mm) was used. The mean signal intensity (Sl₀) values were calculated on regions of interest (ROI) manually drawn on the liver, muscle, spleen, cortical regions of kidneys and in HBV-Tg mice on the neoplastic lesions. The measured SI was normalized to a standard Gd(III) solution, in an external reference tube, to take into account differences in the absolute signal intensity values among different images obtained after mice repositioning into the MRI scanner. The normalization was carried out by dividing the SI₀ values of the ROI drawn on the tumor by the SI values of the ROI drawn inside the reference tube (SI_{ref}).

$$SI\ normalized (SI_n) = SI_0/SI_{ref}$$

Mean SI enhancement (percentage enhancement) of target tissues (TT) was calculated according to the following equation:

SI%Enhancement = [
$$\left(\text{mean SI}_n(TT)\text{post}t\text{-contrast}\right)$$

-mean $\left(\text{SI}_n(TT)\text{pre}-\text{contrast}\right)$
/mean $\left(\text{SI}_n(TT)\text{pre}-\text{contrast}\right) \times 100$

SNR and CNR were calculated as follows:

$$SNR = SI_{TT}/6_n$$

where SI_{TT} is the signal intensity measured on a ROI outlined on a target tissue region and 6_n is the standard deviation (SD) of an ROI drawn in the air outside the animal.

$$CNR = (SI_{les} - SI_{liver})/6_n$$

where SI_{les} and SI_{liver} are neoplastic lesions and liver SI, respectively. Student's t-test was used to compare the differences between groups. A p-value < 0.05 was considered statistically significant.

4.9. Ex Vivo Mn Concentration Measurements

Manganese concentration in liver was determined using ICP-MS (Element-2; Thermo-Finnigan, Rodano, Milan, Italy). Sample digestion was performed with 3 ml of concentrated HNO₃ (70%) under microwave heating (Milestone MicroSYNTH Microwave Labstation).

Acknowledgments

The authors gratefully acknowledge Professor Sebastiano Colombatto for rat hepatocyte isolation and EU Action COST D38. This work was supported by MIUR (PRIN 2007W7M4NF) and Nano IGT project (Bando Converging Technologies, Regione Piemonte), ENCITE project (FP7-HEALTH-2007-A) and Hungarian Science Foundation, PD-OTKA-83253.

REFERENCES

- Sanyal AJ, Yoon SK, Lencioni R. The etiology of hepatocellular carcinoma and consequences for treatment. Oncologist 2010: 15: 14–22.
- Lencioni R, Chen XP, Dagher L, Venook AP. Treatment of intermediate/advanced hepatocellular carcinoma in the clinic: how can outcomes be improved? Oncologist 2010; 15(suppl 4): 42–52.
- Digumarthy SR, Sahani DV, Saini S. MRI in detection of hepatocellular carcinoma (HCC). Cancer Imag 2005; 5: 20–24.
- Shimofusa R, Ueda T, Kishimoto T, Nakajima M, Yoshikawa M, Kondo F, Ito H. Magnetic resonance imaging of hepatocellular carcinoma: a pictorial review of novel insights into pathophysiological features revealed by magnetic resonance imaging. J Hepatobil Pancreat Sci 2010; 17: 583–589.
- Edelman RR, Siegel JB, Singer A, Dupuis K, Longmaid HE. Dynamic MR imaging of the liver with Gd-DTPA: initial clinical results. Am J Roentgenol 1989; 153: 1213–1219.
- Seale MK, Catalano OA, Saini S, Hahn PF, Sahanl DV. Hepatobiliaryspecific MR contrast agents: role in imaging the liver and biliary tree. Radiographics 2009; 29: 1725–1748.
- Ito K. Hepatocellular carcinoma: conventional MRI findings including gadolinium-enhanced dynamic imaging. Eur J Radiol 2006; 58: 186–199.
- 8. Leonhardt M, Keiser M, Oswald S, Kühn J, Jia J, Grube M, Kroemer HK, Siegmund W, Weitschies W. Hepatic uptake of the magnetic resonance imaging contrast agent Gd–EOB–DTPA: role of human organic anion transporters. Drug Metab Dispos 2010; 38: 1024–1028.
- Pascolo L, Cupelli F, Anelli PL, Lorusso V, Visigalli M, Uggeri F, Tiribelli C. Molecular mechanisms for the hepatic uptake of magnetic resonance imaging contrast agents. Biochem Biophys Res Commun 1999; 257: 746–752.

- Narita M, Hatano E, Arizono S, Miyagawa-Hayashino A, Isoda H, Kitamura K, Taura K, Yasuchika K, Nitta T, Ikai I, Uemoto S. Expression of OATP1B3 determines uptake of Gd–EOB–DTPA in hepatocellular carcinoma. J Gastroenterol 2009; 44: 793–798.
- 11. Wang J, Pantopoulos K. Regulation of cellular iron metabolism. Biochem J 2011; 434: 365–381.
- Arosio P, Ingrassia R, Cavadini P. Ferritins: a family of molecules for iron storage, antioxidation and more. Biochim Biophys Acta 2009; 1790: 589–599.
- Li JY, Paragas N, Ned RM, Qiu A, Viltard M, Leete T, Drexler IR, Chen X, Sanna-Cherchi S, Mohammed F, Williams D, Lin CS, Schmidt-Ott KM, Andrews NC, Barasch J. Scara5 is a ferritin receptor mediating nontransferrin iron delivery. Dev Cell 2009; 16: 35–46.
- 14. Troadec MB, Ward DM, Kaplan J. A Tf-independent iron transport system required for organogenesis. Dev Cell 2009; 16: 3–4.
- Huang J, Zheng DL, Qin FS, Cheng N, Chen H, Wan BB, Wang YP, Xiao HS, Han ZG. Genetic and epigenetic silencing of SCARA5 may contribute to human hepatocellular carcinoma by activating FAK signaling. J Clin Invest 2010; 120: 223–241.
- Kálmán FK, Geninatti-Crich S, Aime S. Reduction/dissolution of a beta-MnOOH nanophase in the ferritin cavity to yield a highly sensitive, biologically compatible magnetic resonance imaging agent. Angew Chem Int Edn Engl 2010; 49: 612–615.
- 17. Chisari FV, Pinkert CA, Milich DR, Filippi P, McLachlan A, Palmiter RD, Brinster RL. A transgenic mouse model of the chronic hepatitis B surface antigen carrier state. Science 1985; 230: 1157–1160.
- Barone M, Spano D, D'Apolito M, Centra M, Lasalandra C, Capasso M, Di Leo A, Volinia S, Arcelli D, Rosso N, Francavilla A, Tiribelli C, lolascon A. Gene expression analysis in HBV transgenic mouse liver: a model to study early events related to hepatocarcinogenesis. Mol Med 2006; 12: 115–123.
- Dunsford HA, Sell S, Chisari FV. Hepatocarcinogenesis due to chronic liver cell injury in hepatitis B virus transgenic mice. Cancer Res 1990; 50: 3400–3407.
- Pastor CM, Planchamp C, Pochon S, Lorusso V, Montet X, Mayer J, Terrier F, Vallee JP. Kinetics of gadobenate dimeglumine in isolated perfused rat liver: MR imaging evaluation. Radiology 2003; 229: 119–125.
- 21. Ayyappan AP, Jhaveri KS. CT and MRI of hepatocellular carcinoma: an update. Expert Rev Anticancer Ther 2010; 10: 507–519.

- Roskams T, Kojiro M. Pathology of early hepatocellular carcinoma: conventional and molecular diagnosis. Semin Liver Dis 2010; 30(1): 17–25.
- Aime S, Aime S, Delli Castelli D, Geninatti Crich S, Gianolio E, Terreno E. Pushing the sensitivity envelope of lanthanide-based magnetic resonance imaging (MRI) contrast agents for molecular imaging applications. Acc Chem Res 2009; 42: 822–831.
- 24. Caravan P. Strategies for increasing the sensitivity of gadolinium based MRI contrast agents. Chem Soc Rev 2006; 35: 512–523.
- Geninatti Crich S, Bussolati B, Tei L, Grange C, Esposito G, Lanzardo S, Camussi G, Aime S. Magnetic resonance visualization of tumor angiogenesis by targeting neural cell adhesion molecules with the highly sensitive gadolinium-loaded apoferritin probe. Cancer Res 2006; 66: 9196–9201.
- Fries PH, Belorizky E. Enhancement of the water proton relaxivity by trapping Gd3+ complexes in nanovesicles. J Chem Phys 2010; 133: 024504.
- Sánchez P, Valero E, Gálvez N, Domínguez-Vera JM, Marinone M, Poletti G, Corti M, Lascialfari A. MRI relaxation properties of water-soluble apoferritin-encapsulated gadolinium oxide-hydroxide nanoparticles. Dalton Trans 2009; 5: 800–804.
- Kim JH, Kim MJ, Park YN, Lee JT, Kim BR, Chung JB, Choi JS, Kim KS, Kim KW. Mangafodipir trisodium-enhanced MRI of hepatocellular carcinoma: correlation with histological characteristics. Clin Radiol 2008; 63: 1195–1204.
- Planchamp C, Montet X, Frossard JL, Quadri R, Stieger B, Meier PJ, Ivancevic MK, Vallée JP, Terrier F, Pastor CM. Magnetic resonance imaging with hepatospecific contrast agents in cirrhotic rat livers. Invest Radiol 2005; 40: 187–194.
- Di Tommaso L, Destro A, Seok JY, Balladore E, Terracciano L, Sangiovanni A, lavarone M, Colombo M, Jang JJ, Yu E, Jin SY, Morenghi E, Park YN, Roncalli M. The application of markers (HSP70 GPC3 and GS) in liver biopsies is useful for detection of hepatocellular carcinoma. J Hepatol 2009; 50: 746–754.
- Bradford MMA. rapid and sensitive method for the quantitation of microgram quantities of protein utilizing the principle of proteindye binding. Anal Biochem 1976; 72: 248–254.
- Gardini G, Cabella C, Cravanzola C, Vargiu C, Belliardo S, Testore G, Solinas SP, Toninello A, Grillo MA, Colombatto S. Agmatine induces apoptosis in rat hepatocyte cultures. J Hepatol 2001; 35: 482–489.